THE EFFECT OF FINAL HEAT TREATMENT AT FABRICATION ON THE TERMINAL SOLID SOLUBILITY OF HYDROGEN IN ZRY-4

A. YAMAUCHI, M. AMAYA
Nuclear Safety Research Center, Japan Atomic Energy Agency
Tokai-mura, Naka-gun, Ibaraki 319-1195 - Japan

ABSTRACT

Differential scanning calorimetry (DSC) measurements on pre-hydrided cold worked, stress relieved and recrystallized Zry-4 cladding were performed in a temperature range from 50 to 600°C in order to elucidate the effect of final heat treatment at fabrication of Zircaloy-4 (Zry-4) cladding on the terminal solid solubility during the dissolution of zirconium hydrides at heating up (TSSD). Obtained DSC curves and optical micrographs indicate that the initial morphology of hydrides affects the dissolution behavior of hydride. The Arrhenius plots between the TSSD temperatures and hydrogen contents obtained in this study revealed that cold worked samples exhibited the largest TSSD and followed by stress relieved and recrystallized samples. The results of this study indicated that the difference in microstructure due to final heat treatment at fabrication of Zry-4 cladding affects the dissolution behavior of hydrides during heating up.

1. Introduction

It is well known that zirconium (Zr) alloy components are easy to pick up hydrogen which is generated mainly by their surface corrosion during reactor operation[1]. If the hydrogen content reaches the terminal solid solubility of hydrogen (TSS) in Zr alloy, hydrogen precipitates as zirconium hydride phase. Zirconium hydride is brittle, and significant precipitation of zirconium hydrides is likely to degrade of mechanical property of Zr alloy components. Crackings of Zr alloy components caused by precipitation of hydrides, *e.g.* delayed hydride cracking of pressure tube in CANDU type reactor[2,3] and outside-in type cracking in high burnup BWR fuel cladding during power ramp test[4,5], has been reported.

TSS of hydrogen in Zr alloy is important as fundamental data for a prediction of dissolution and precipitation behavior of hydrides. While it is considered that fabrication processes of Zr alloy components, *e.g.* final heat treatment might affect a behavior of hydride in a material, few studies have been carried out on a relationship between fabrication condition and dissolution or precipitation behavior of hydrides in Zr alloy[6].

Differential scanning calorimetry (DSC) is one of the technique that has been used to investigate TSS in Zr alloy[7-14]. In this study, in order to elucidate the effect of final heat treatment at fabrication of Zircaloy-4 (Zry-4) cladding on the terminal solid solubility during dissolution of zirconium hydrides at heating up (TSSD), DSC measurements were performed on pre-hydrided cold worked (CW), stress relieved (SR) and recrystallized (RX) Zry-4 cladding materials in a temperature range from 50 to 600°C.

2. Experimental

2.1 Samples

Samples for this study were prepared by cutting from non-irradiated Zry-4 cladding tubes. The sample size was roughly 2 mm in thickness and 3 mm in width, and the sample weight was about 25 mg. The cladding tubes were produced using a commercial fabrication process for a PWR fuel cladding tube, and two kinds of final heat treatments were conducted to prepare the cladding tubes with RX and SR conditions. The CW tubes were also used in this study for comparison.

The three types of cladding tubes were then pre-hydrided by two methods. One was gaseous hydrogenation at 400 ^{o}C in an Ar/3%H_2 mixed gas for 90 or 120 minutes. The other was hydrogenation by a corrosion reaction in an aqueous solution of LiOH at 330^{o}C for 11 or 15 hours. The former method was applied to prepare lower hydrogen content cladding tubes (<200 ppm), and the latter method for higher hydrogen content cladding tubes (>200 ppm). Hydrogen contents of the cladding tubes ranged from 8.6 to 423.2 wppm, as measured with a LECO RHEN-602. Table 1 lists the measured hydrogen contents for each cladding tubes, and Fig. 1 shows the optical micrographs of cross section of the CW, SR and RX cladding tubes that contain about 200 wppm of hydrogen. From these micrographs, the effect of the final heat treatment on the morphology of precipitated hydrides is found: fine hydrides are observed in the CW cladding tube and some of those congregate and form longer hydrides. In the SR cladding tube, hydrides are precipitated mainly along the circumferential direction. As for the RX cladding tube, hydrides precipitated along radial direction are also observed.

Table 1 List of the samples used in this study

	sample	Final Heat treatment	H-content (wppm)
1	2-CW-AR	CW	8.6
2	2-CW-1	CW	203.5
3	2-CW-3	CW	370.7
4	2-CW-4	CW	413.2
5	2-SR-AR	SR	9.8
6	SRQ1007.1	SR	80.4
7	2-SR-1	SR	205.5
8	2-SR-3	SR	356.0
9	2-SR-4	SR	423.2
10	2-RX-AR	RX	8.6
11	RXQ1017.2	RX	173.5
12	2-RX-1	RX	212.0
13	2-RX-3	RX	355.4
14	2-RX-4	RX	409.0

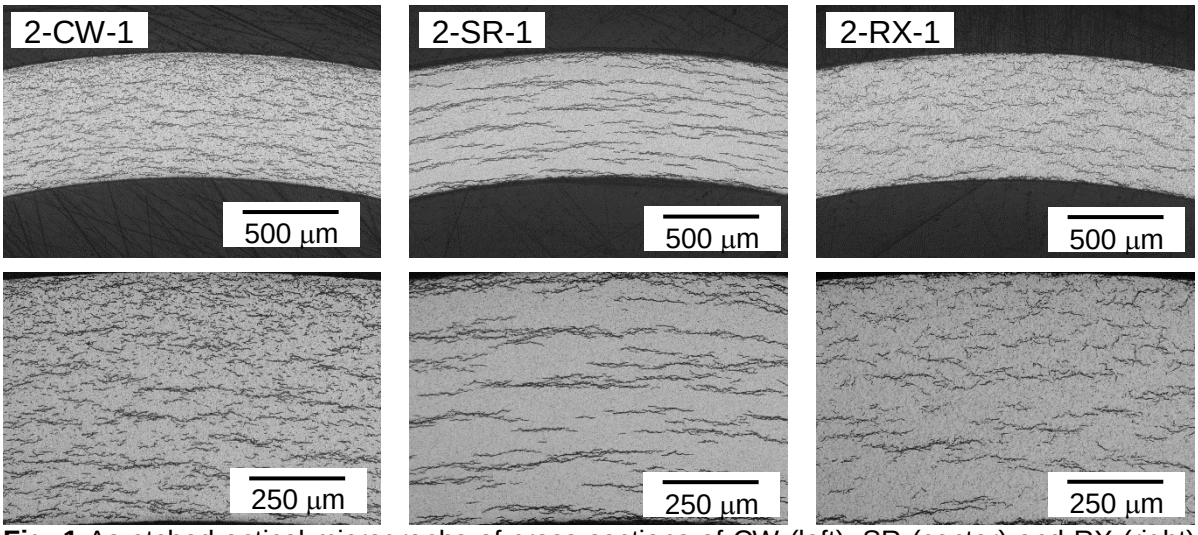

Fig. 1 As-etched optical micrographs of cross sections of CW (left), SR (center) and RX (right). The gray lines and dots are precipitated hydrides. The hydrogen contents of the cladding tubes were 203.5, 205.5 and 212.0, respectively.

2.2 Differential scanning calorimetry (DSC)

Hydride dissolution behavior during heating up was investigated using DSC technique. A simultaneous thermal analyzer, Netzsch STA449 F3, was used in this study. A measuring part consists of a furnace and a sensor with sample and reference pans made of platinum. The temperatures at the sample and reference pans are measured with the thermocouples connected to each sensor area under a certain constant heating rate controlled by the furnace. The reference pan is usually empty, and the heat flow into the sample pan can be evaluated from the temperature difference between the sample and reference pans. When the dissolution of hydride in the sample, of which reaction is endothermic, occurs, a peak is observed in a time-heat flow curve.

The DSC measurements were carried out under a pure Ar gas flow of 30 ml/min to prevent sample oxidation. The temperature range of the measurement was from 50 to 600 ^{o}C. The heating rate was 20 ^{o}C/min. After the temperature reached the maximum temperature (600 ^{o}C), the sample was furnace cooled to room temperature. The measurements were conducted two times per sample.

3. Results and discussion

3.1 DSC curves and dissolution behavior of Zr hydrides

Fig. 2 shows a typical example of a heat flow curve (DSC curve) of the CW sample prepared from the pre-hydrided cladding tube containing 370.7 wppm of hydrogen. The derivative of the DSC curve (DDSC curve) is also shown in the Fig. 2. A broad endothermic peak which corresponds to the dissolution of hydrides in the sample is observed. According to a Zr–H phase diagram[15], dissolution of hydride occurs in a wide range of temperature, thus, no sharp peaks can be observed during hydride dissolution process. In this case, as the temperature increases, the DSC curve gradually deviates from the baseline at around 230^{o}C because a part of the heat absorbed into the sample is used to dissolve hydrides gradually into sample matrix. Then, the DSC curve returns to the baseline at around 490^{o}C and this indicates the completion of dissolution of hydrides.

As for this broad peak, three notable temperatures are seen, *i.e.* the Peak Temperature (PT), the Maximum Slope Temperature (MST) and the Completion Temperature (CT). It seems that no theories have been established for choosing the point in the peak that can be identified with TSSD. However, Une[7,8] and Khatamian[9,10] chose the MST as the TSSD temperature, considering not only that data analysis becomes easy but also that better correlation could be seen between their MST and the reported equilibrium TSSD obtained in the diffusion annealing technique[11]. In order to maintain consistency with previous studies, the MST is taken as TSSD temperature in this study.

Fig. 3 shows the DSC curves of the CW, SR and RX samples. It is found that a part of the samples that have relatively higher hydrogen content exhibit two peaks in the DSC curves. The second peaks in the SR samples were sharper than those in the CW and RX samples. Fig. 4 compares the DSC curves of the SR sample obtained at the first and second run measurements. Although the measurements were carried out on the same samples, the shapes of the DSC curves were different: the DSC curves of the second run measurements show single peaks and the MSTs decreases by about 15 ^{o}C. Before the first run measurement, some hydrides in the sample congregated and formed stacking hydrides (Fig. 5). On the other hand, after the first run measurement, the sizes and distribution of the hydrides seem to become relatively uniform. This change in the hydride morphology may be explained by the homogenization of hydrogen occurred during the heating up of the first run measurement: dissolved hydrogen has higher mobility to distribute itself in Zr matrix. Thus, the hydrides precipitated in a more uniform manner

during the cooling stage. These results shows that the initial morphology of hydrides affects the shape of DSC curve which corresponds to dissolution behavior of hydride in the Zry-4 samples.

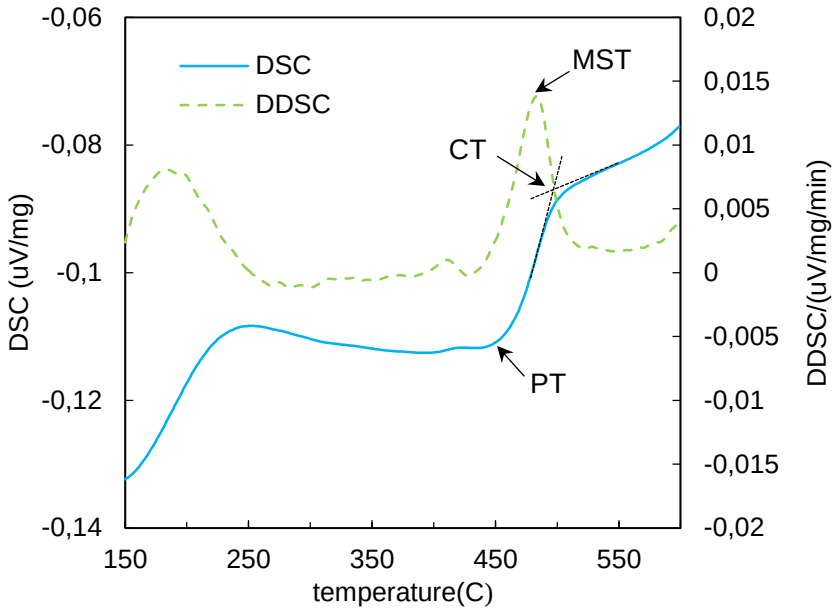

Fig. 2 DSC and DDSC curves of the CW sample obtained during the first run measurement. The sample was taken from the pre-hydrided cladding tube which contains 370.7 wppm hydrogen.

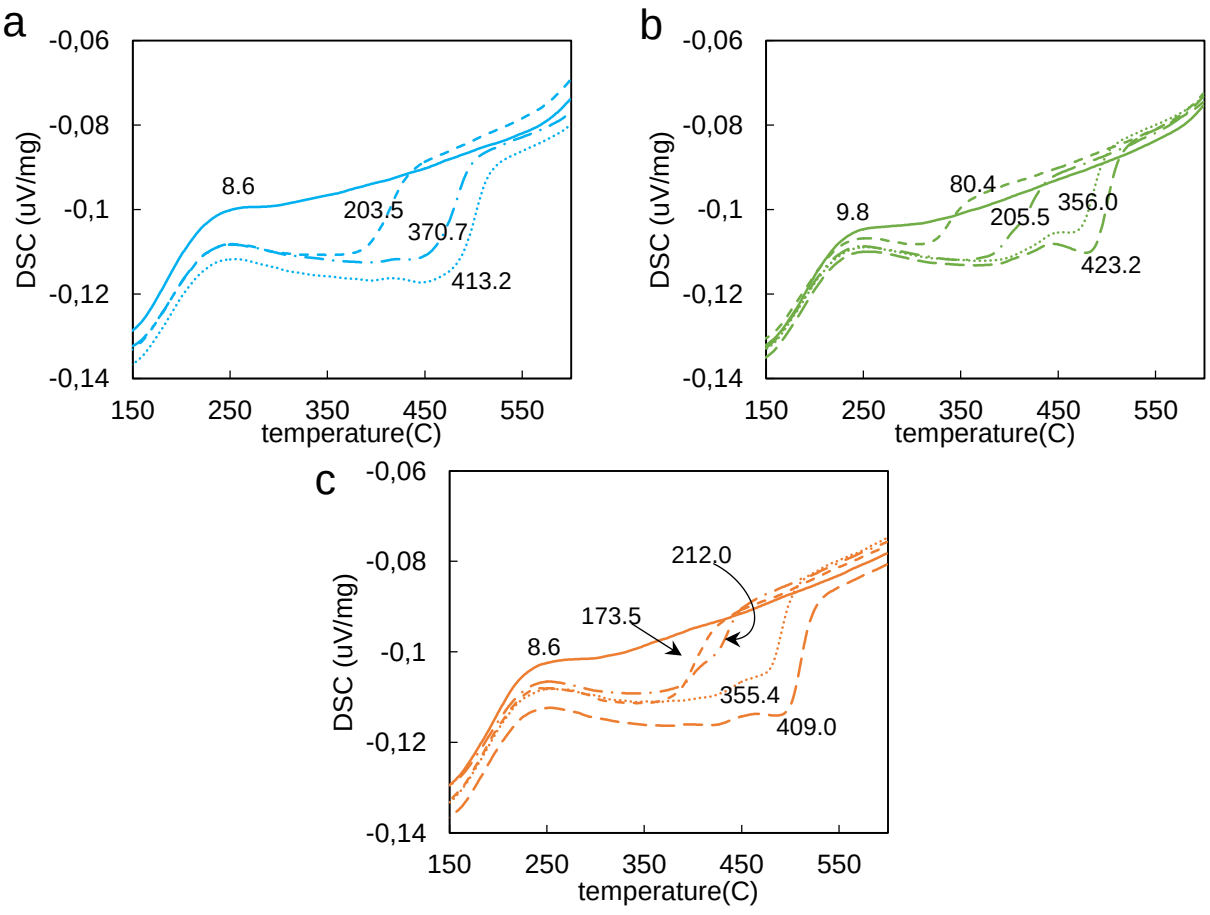

Fig. 3 DSC curves of the samples (a: CW, b: SR and c: RX). The numbers shown in the figure indicate hydrogen contents of the cladding tubes from which the samples were prepared.

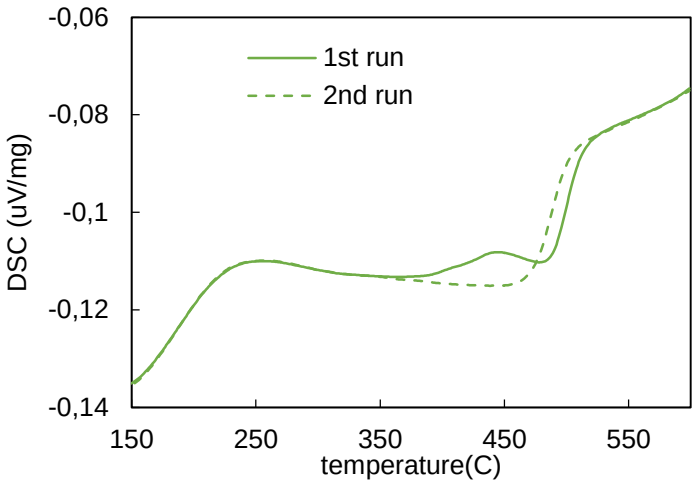

Fig. 4 Comparison between the DSC curves of the SR sample obtained during the first and second run measurements. The hydrogen content in the sample before the first run measurement was evaluated as 423.2 wppm.

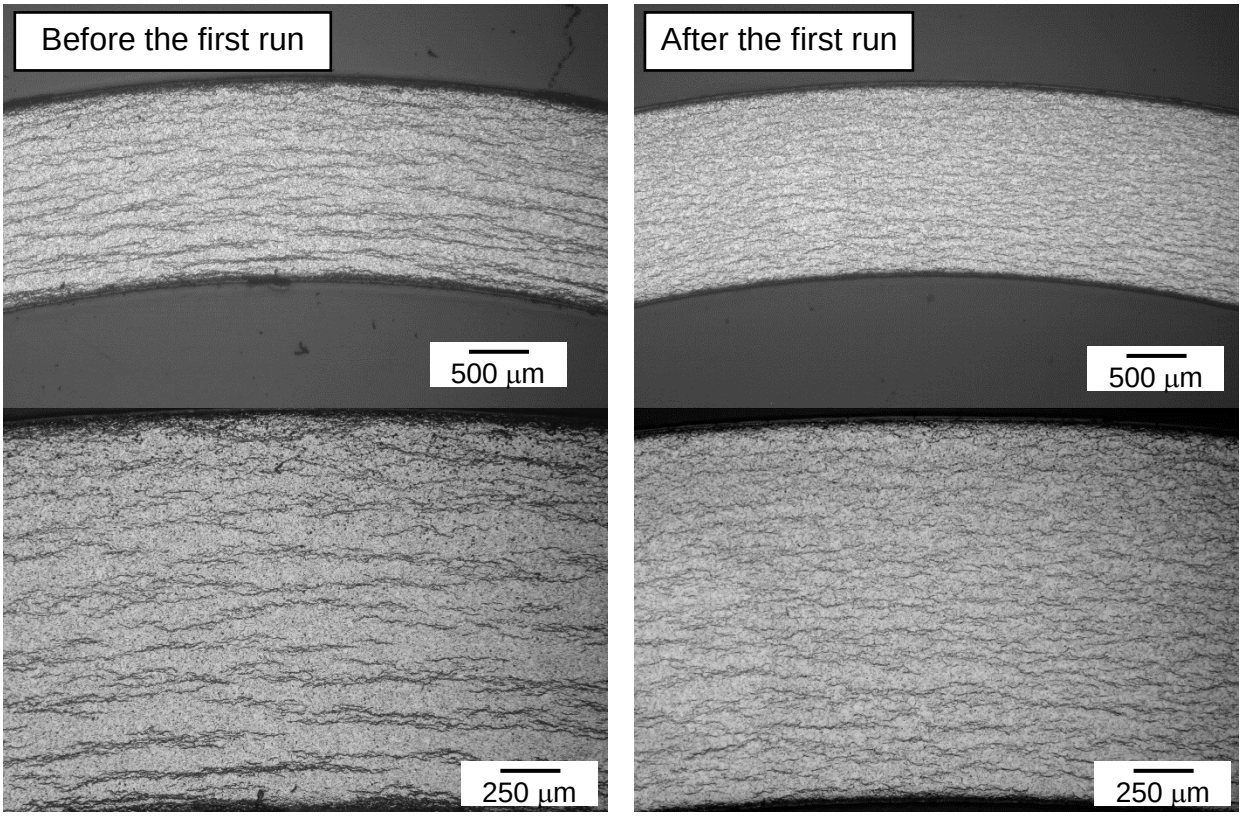

Fig. 5 Comparison between optical micrographs of the SR sample before and after the first run measurement. The maximum temperature during the measurement was 600°C. The average cooling rate from the maximum temperature to room temperature was approximately 10 °C. The hydrogen content of the sample before the first run measurement was evaluated as 423.2 wppm.

3.2 TSSD

The Arrhenius plots between the TSSD temperatures and the hydrogen contents obtained in this study are shown in Fig. 6. Based on these results, the following equations were obtained by linear regression of log C_H (hydrogen content in the sample) on 1/T (reciprocal temperature):

$$C_{H\_CW}(\text{ppm}) = 1.22 \times 10^5 \exp(-36565/\text{R}T), \quad (1)$$

$$C_{H\_SR}(\text{ppm}) = 1.99 \times 10^5 \exp(-39741/\text{R}T), \quad (2)$$

$$C_{H\_RX}(\text{ppm}) = 1.98 \times 10^5 \exp(-40256/\text{R}T), \quad (3)$$

where, R is the gas constant (8.314 J/K/mol); and *T*, the temperature in K. As shown in Fig. 6, the CW samples exhibit the highest TSSD and followed by SR and RX samples. These results indicate that the difference in the microstructure due to final heat treatment at fabrication affects the dissolution behavior of hydrides in Zry-4 cladding tube.

The reason why the CW samples exhibit the highest TSSD may be explained as follows. In the CW samples, more defects and larger compressive stress and strain remain compared with SR and RX samples. These factors could make hydrogen easier to dissolve: defects in the sample e.g. dislocation loops could be preferable sites for hydrogen dissolution and residual compressive stress and strain may provide a portion of energy for hydrogen atom to move into Zr matrix. Similarly, the TSSD of the SR samples could become higher than those of the RX sample because larger residual strain remains in the former sample compared with the latter.

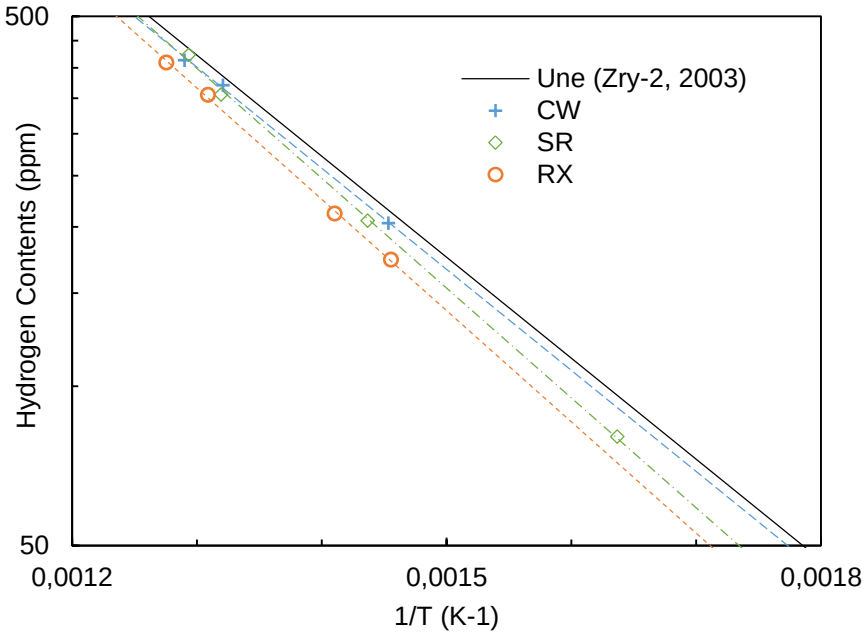

Fig. 6 Arrhenius plots between the TSSD temperatures and hydrogen contents obtained in this study. The TSSD data reported by Une[6], et al. is also shown as a reference.

4. Conclusions

DSC measurements on samples obtained from the CW, SR and RX Zry-4 cladding tubes were performed in a temperature range from 50 to 600°C in order to elucidate the effect of final heat treatment at fabrication of Zry-4 cladding tube on TSSD. Samples for this study were prepared by

cutting from pre-hydrided CW, SR and RX Zry-4 cladding tubes, and the hydrogen contents of the samples ranged from 8.6 to 423.2 ppm. DSC measurements were carried out two times per sample under a heating rate of 20^{o}C/min and a flow rate of pure Ar gas of ~30 ml/min.

The following conclusions were obtained. These findings will be useful to analyze the fuel behavior during an anticipated operational occurrence and a design-basis accident where the behavior of hydrogen in the fuel cladding plays an important role in terms of the fuel failure under such conditions.

- From comparison between the DSC curves obtained in the first and second run measurements, it is suggested that the initial morphology of zirconium hydrides would affect the dissolution behavior of hydride in the Zry-4 samples.
- CW samples exhibited the largest TSSD and followed by SR and RX samples. The results of this study indicated that the difference in microstructure due to final heat treatment at fabrication affects the dissolution behavior of hydrides in Zry-4 cladding tube.
- From the Arrhenius plots of the TSSD temperatures and hydrogen contents, TSSD for CW, SR and RX samples were formulated as below:

$$C_{H\_CW}(\mathrm{ppm}) = 1.22 \times 10^{5}\exp(-36565/\mathrm{R}T)$$

$$C_{H\_SR}(ppm) = 1.99 \times 10^{5}\exp(-39741/\mathrm{R}T)$$

$$C_{H\_RX}(ppm) = 1.98 \times 10^{5}\exp(-40256/\mathrm{R}T)$$

References

[1] Corrosion of Zirconium Alloys in Nuclear Power Plants, IAEA-TECDOC-684,Vienna, 1993.
[1] D.O. Northwood, U. Kasasih, Int. Met. Rev. 28 (1983) 92.
[2] B. Cox, J. Nucl. Mater. 170 (1990) 1.
[3] Summary Report on The Verification Test on BWR High Burnup Fuel, Nuclear Power Engineering Corporation (NUPEC), March 2002.
[4] S. Shimada, et al., J. Nucl. Mater, 327 (2004) 2.
[5] J.J. Kearns, J. Nucl. Mater. 22 (1967) 292.
[6] K. Une, S. Ishimoto, J. Nucl. Mater. 322 (2003) 66.
[7] K. Une, et al., J. Nucl. Mater. 389 (2009) 127.
[8] D. Khatamian, et al., J. Alloy Comp. 231 (1995) 488.
[9] D. Khatamian, V.C. Ling, J. Alloy Comp. 253 (1997) 162.
[10] P. Vizcaíno, et al., J. Nucl. Mater. 304 (2002) 96.
[11] D. Khatamian, J. Alloy Comp. 356 (2003) 22.
[12] D. Setoyama et al., J. Nucl. Mater. 344 (2005) 291.
[13] M. Ito, et al., J. Alloy Comp. 446 (2007) 451.
[14] T. B. Massalski, et al., Binary Alloy Phase Diagram, Second Edition, ASM (1990)